LOW COST AC-AC DRIVE FOR HOUSEHOLD APPLIANCES: DESIGN METHODOLOGY OF POWER STAGE

Romeu Antunes Friedemann.
Federal University of Santa Catarina (UFSC)
Power Electronics Institute (INEP).
P.O. Box 5119 88040-970.
Florianópolis, SC – Brazil.
romeuaf@gmail.com

Ivo Barbi.
Federal University of Santa Catarina (UFSC)
Power Electronics Institute (INEP).
P.O. Box 5119 88040-970.
Florianópolis, SC – Brazil.
ivobarbi@inep.ufsc.br

Abstract – This paper presents the design methodology of an AC-AC converter applied to drive single-phase induction motors in household appliances. The converter can be fed by wide range input voltages. The topology was chosen based mainly on the cost. The design methodology is presented, and the peculiar characteristics and implications are discussed. The main contribution of this paper is the presentation of a methodology to determine capacitor's value from typical project parameters. Finally, some experimental results are shown and also discussed.

Keywords - AC-AC Converter, Drive, Household Appliances, Reduced Capacitor Link, Harmonics.

I. INTRODUCTION

The use of single-phase induction motors in household appliances (generally at low power loads) is widely spread by the industries. However, the different values of supply voltage makes necessary to adapt the equipments according to the consumption's level.

It is very common to find transformers connected to the input supply of refrigerators, air-conditioners and other devices, to regulate the voltage level of input. This is the AC-voltage regulators simplest solution. But it has low efficiency due to the reactive energy demanded by transformer, and also, because the transformer is never turned off. So, the integration of low cost AC-voltage regulators with household devices is a tendency, creating one complete solution for customers.

The purpose of this paper is to present the design methodology of an AC-AC converter, which is already known in the literature, applied to drive household devices fed by wide range voltage systems. Several AC-AC converters topologies have been proposed in literature. Based on factors such as load power, power quality, efficiency, and mainly, the cost, one was chosen for the prototype implementation, being presented advantages and drawbacks.

The principle of an AC-voltage regulator is to control the fundamental voltage value supplied to the load. Basically, this can be done in three different ways:

- Phase angle control;
- Integral cycle control;
- High frequency PWM duty-cycle control.

The first one uses just a triac or two thyristors, which offers a lower cost solution, with reduced number of component and simplified command circuit. The drawbacks are the high levels of harmonic content on the load side, and on the input supply side too. A different way to control the RMS output voltage using the same circuit is through the Integral Cycle Control. Hence, this technique introduces subharmonic components, causing torque oscillations, acoustic noises and other disturbances. Last technique can be used instead, reducing passive elements' volume, the total harmonic distortion and consequently, improving the power factor of AC-regulator.

Frequency converters have already been used [1] to drive refrigerators. However, such as explained, this is not a cheap solution yet.

Direct converters are investigated in [2-7]. A family of AC choppers is presented in [2] and [3], and its derivations are found in [4] and [5]. Different switching techniques are proposed in [6] and [7]. Common drawbacks of these structures are the commutation problems, related to the dead time, and voltage spikes that must be controlled.

On the other hand, some structures of indirect converters with reduced energy storage in the DC link have been proposed [8-14]. In [8] and [9], two converters with quasi-direct link are discussed. An AC-AC converter with direct link is found in [13] and its derivation in [14], using bidirectional switches on the output inverter and also on the input rectifier. Lower cost converters are presented in [10], [11] and [12] using a simple full bridge diode circuit as input rectifier. The advantages of these converters related to the AC choppers are the elimination of the commutation problems and simpler command circuits.

The design methodology discussed in this paper refers to the topology proposed in [10]. It was implemented in a prototype [12], and some results are shown and discussed. This structure was chosen due to the low cost compared to the bidirectional input topologies, and also because it uses a simpler command scheme.

II. GENERALITIES

The implemented structure can be viewed in Fig. 1. It seems like a frequency converter, but the main difference consists in the fact of DC link voltage (v_{DC}) has the rectified sinusoidal waveform, due to the capacitor link be around some μF.

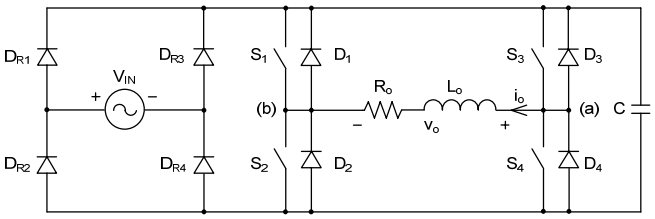

Fig. 1. Schematic of DC link AC voltage regulator implemented.

This leads to adopt an RPWM (Rectangular Pulse Width Modulation) modulation scheme. In [10], a modified scheme of modulation is proposed, in order to reduce the commutation power losses. It is an interesting strategy allied to digital control.

The converter has two different ways of operation: energy transference from the input line to the load, and energy recovery from the load to DC link capacitor. The first one occurs on the first and third quadrants (depending on the half cycle of input voltage) while the second occurs on the second and fourth quadrants. Therefore, v_{DC} is distorted during the energy recovery, needing a feedforward loop to compensate the distortion effects over the load.

An analog control was used in this study so, symmetrical power supplies were necessary. Therefore, the traditional unipolar modulation scheme was implemented, and the input voltage signal detector proposed in [10] could be suppressed. Fig. 2 shows the implemented feedforward loop:

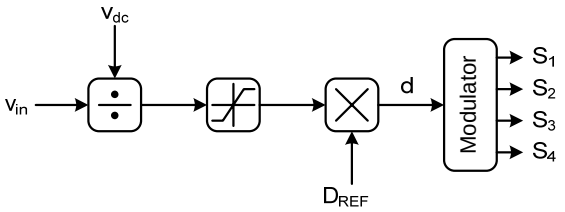

Fig. 2 – Implemented feedforward loop.

The reference duty cycle (D_{REF}) is reduced according to (1), by the ratio between input voltage (v_{IN}) and v_{DC}, during the energy recovery from the load to DC link capacitor. As result, the fundamental voltage waveform remains sinusoidal.

$$d = D_{REF} \cdot \frac{v_{IN}}{v_{DC}} \tag{1}$$

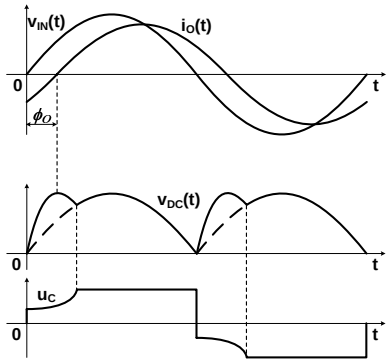

Fig. 3 – Waveforms of converter.

On top, Fig. 3 presents input voltage and output current. On bottom, v_{DC} and the real duty cycle (d) are shown. The angle between input voltage and output current is ϕ_O.

III. DESIGN METHODOLOGY

A. Capacitor Determination

The most important converter component is the DC link capacitor. This component has the function of storing energy during the recovery energy from load. Once its value has been defined, the converter behavior must be comprehended against operation point variations. KRAGH [10] presents the equation to determine capacitor's value (3) starting from the energy balance equation (2). But (3) depends on parameters such as output inductance, output resistance and load current. The main contribution of this paper is the presentation of a methodology to determine capacitor's value from typical project parameters, such as RMS voltage input, load power, cos (ϕ_O), and the maximum admissible DC link voltage.

$$\frac{1}{2}.L_O.{i_O}^2(t) = \frac{1}{2}.C.{v_{DC}}^2(t) + \int_0^{t_f} R_O.{i_O}^2(t)\,dt \tag{2}$$

$$C = \frac{L_O.{I_O}^2(0) - R_O.{I_{O\_PK}}^2.\left(t_F - \frac{sen(\omega_R.t_F).cos(\omega_R.t_F)}{\omega_R}\right)}{{V_{DC\_PK}}^2} \tag{3}$$

Where:

L_O - Output equivalent inductance.
R_O - Output equivalent resistance.
$I_O(0)$ - Load current at initial time (t_O), when $v_O(t)$ is zero.
I_{O_PK} - Peak of load current.
V_{DC_PK} - Maximum voltage at DC link, occurs at final time (t_F), when $i_O(t)$ is zero.
ω_R - angular frequency input.
$\omega_R.t_F$ - angle ϕ_O, between v_{IN} and i_O.

So, a parameterized equation (4) to design the DC link capacitor is found. The process to obtain it is too long, for this reason it is not presented here. More details are given [12].

$$\overline{\overline{C}} = \left(\frac{1}{A}\right)^2 .\left(tan\phi_O - \phi_O\right) \tag{4}$$

Where:

$$A = \frac{V_{DC\_PK}}{V_{IN\_PK}} \tag{5}$$

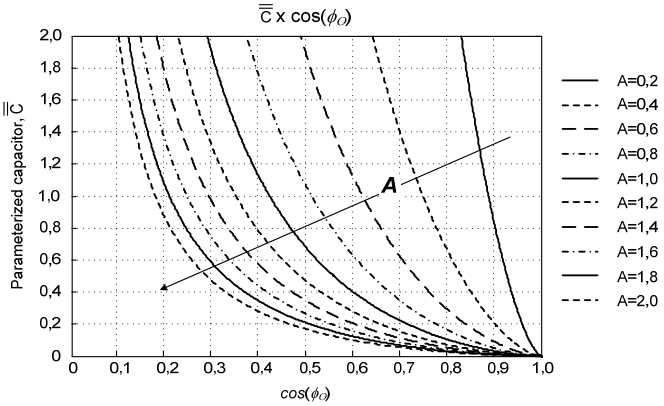

Fig. 4 – Parameterized curves of $\overline{\overline{C}}$.

Equation (4) is represented graphically in Fig. 4. It shows the variations of A, and therefore of V_{DC_PK}, *versus* $cos(\phi_O)$ and $\overline{\overline{C}}$.

In (5), it is defined the ratio between the maximum value of v_{DC}, called V_{DC_PK} (during the energy recovery) and the peak value of input voltage (V_{IN_PK}). The first one must be specified, and the second is a known data. The angle ϕ_O is

also a known data. The parameterized capacitor link value is represented by $\overline{\overline{C}}$. Finally, the capacitor value is obtained from data project using (6), where P_O is the output active power (load power), and f_R is the line frequency input.

$$C = \overline{\overline{C}}.\frac{P_O}{2.\pi.f_R.v_{IN\_RMS}^{\ 2}} \quad (6)$$

B. Converter Behavior

Once the capacitor link has been defined, it becomes interesting to know the effects of its choice over the converter.

In fact, V_{DC_PK} depends basically on the load, through P_O and ϕ_O. It depends also on the duty cycle, according to (7), which represents the operation point:

$$\overline{\overline{C}} = \frac{Z_O}{Z_C}.\frac{1}{D^2} \quad (7)$$

Z_O is the nominal impedance of load in the input line frequency (f_R), and Z_C is the DC *link* impedance ($1/2\pi.f_R.C$). It means that the nominal value of $\overline{\overline{C}}$, established at nominal operation point, is affected by the ratio $1/D^2$. Additionally, the phase angle ϕ_{IN}, between input current (i_{IN}) and v_{IN} is also affected by the same ratio, as follow (8):

$$\phi_{IN} = tan^{-1}\left(tan\phi_O - \frac{Z_O}{Z_C}.\frac{1}{D^2}\right) \quad (8)$$

It is demonstrated (9) that the angle added by capacitor C to ϕ_O, called α_{DC}, depends on project data and also on the operation point. Fig. 5 represents graphically the α_{DC} variation:

$$\alpha_{DC} = tan^{-1}\left(\frac{Z_O}{Z_C}.\frac{1}{D^2}\right) \quad (9)$$

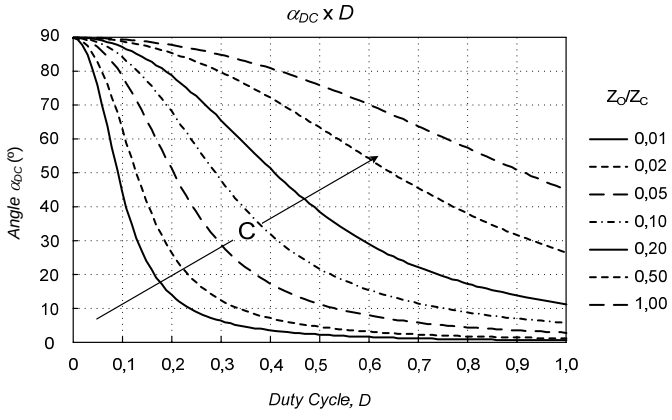

Fig. 5 – Phase angle α_{DC} added to ϕ_O, *versus* duty cycle *D*.

C. Input Current Distortion

$$THDi_{IN} = \sqrt{\frac{\sum_{n=2}^{\infty}\left\{\left(\frac{sen\left[(n-1)\gamma\right]}{n-1}\right)^2 + \left(\frac{sen(n.\gamma)}{n}\right)^2 + \frac{2.sen\left[(n-1)\gamma\right].sen(n.\gamma)}{(n-1).n}.cos(\phi_{IN}-\beta)\right\}}{\gamma^2 + sen^2\gamma + 2.\gamma.sen\gamma.cos(\phi_{IN}-\beta)}} \quad (10)$$

$$\gamma = \left(\pi - \phi_{IN} - \beta\right) \quad (11)$$

The Total Harmonic Distortion (*THD*) of the i_{IN} can be obtained by an analytical expression (10), where γ is the conduction angle of input rectifier, defined by (11), and β is the complementary angle to ϕ_{IN}, when rectifier is blocked.

These expressions have low practical interest due to their dependence on parameters *D*, γ, ϕ_{IN} e β. Instead, is more interesting to obtain the input current *THD* by simulations at nominal operation points.

In order to filter the high frequency harmonic content, a low value inductance can be added in series with the input rectifier, called L_{IN}. The criteria of resonance frequency (f_O) between L_{IN} and C must be considered to calculate L_{IN}'s value:

$$L_{IN} = \frac{1}{\left(2\pi f_O\right)^2 C} \quad (12)$$

In practical terms, the stray inductances of line are great enough to reduce these harmonic components in high frequencies in most part of applications.

D. Control Structure

To control RMS output voltage, a structure of slow controller can be used, without any drawback to the motor operation. This is possible because the mechanical responses are slower than electrical. The block diagram of implemented control is shown in Fig. 6. The system model is represented by a gain, equal to D in the perturbation input side, and equal to the RMS input value in the reference input side. The measured signal v_{O_RMS}' is a DC signal proportional to the RMS output value of fundamental component, and the reference V_{REF} is adjusted to obtain the desired output voltage. H_1 and H_2 are respectively, a low pass filter to eliminate the high frequency content of output voltage, and an RMS to DC converter circuit. G_{PWM} is the modulator gain, and G_{PB} is a low pass filter after the feedforward loop.

The designed control must be stable for variations on the load current and on the input voltage too, considering that the converter input is connected to a wide range voltage system. It was designed according to Table I, with 110V and 220V as the RMS input values. As explained, these are the system gains, illustrated in Fig. 6. G_{PB} must be adjusted to filter switching frequency noises, with no influence in fundamental frequency phase. The same is applied to H_1.

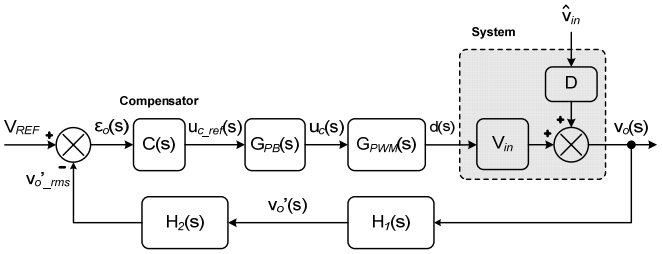

Fig. 6 – Control structure: block diagram.

Related to the compensator, a phase-delay topology could be used, because its simplicity. Static gain is adjusted with the minor input voltage, to obtain an output voltage error in accordance with Table I. On the other hand, the cut frequency must be adjusted in order to guarantee the system stability in worst case, which is, with the major input voltage.

E. Design Example

The specifications of implemented prototype are found in Table I. FD_O is equal to the $cos(\phi_O)$, f_R is the frequency of input line and f_S is the switching frequency.

Table I
Design Specifications

v_{IN_RMS}	D_{REF}	v_{O_RMS}	V_{DC_PK}	P_O	FD_O	f_R	f_S
110V	1,0	110V/±5%	500V	500W	0,6	60Hz	20kHz
220V	0,5						

The first element to be calculated is capacitor C. The greater one of the feeding voltages can be chosen to determine its value, and the maximum voltage at the DC link will be equal in both cases. From (5), *A* is found:

$$A = \frac{V_{DC\_PK}}{V_{IN\_PK}} = \frac{500V}{\sqrt{2}*220V} = 1,607 \qquad (13)$$

The phase angle ϕ_O is 53,13º, then $\overline{\overline{C}}$ for v_{IN_RMS} equal 220V at nominal operation point is found according to (4):

$$\overline{\overline{C}} = \left(\frac{1}{A}\right)^2.\left(tan\phi_O - \phi_O\right) = \left(\frac{1}{1,607}\right)^2. \qquad (14)$$
$$.\left[tan\left(0,9273rad\right) - 0,9273rad\right] = 0,157$$

Finally, C value is calculated:

$$C = \frac{\overline{\overline{C}}.P_O}{2.\pi.f_R.v_{IN\_RMS}^{\ 2}} = \frac{0,157.500W}{2.\pi.60Hz.\left(220V\right)^2} = \boxed{4,5\mu F} \qquad (15)$$

To specify the switches, (16) to (20) can be used, otherwise, simulations instead. Equations (16) to (19) represent the medium and RMS currents on the switches and diodes, respectively, with the ratio given in (20):

$$\overline{\overline{I_{S\_med1,2,3,4}}} = \frac{I_{S\_med1,2,3,4}}{I_{ref}} = D.\frac{\left(1+D.cos\phi_O\right)}{2\pi} \qquad (16)$$

$$\overline{\overline{I_{S\_RMS1,2,3,4}}} = \frac{I_{S\_RMS1,2,3,4}}{I_{ref}} = \frac{D}{2}.\sqrt{\frac{(1+D)}{2} - D.\left(\frac{\phi_O}{\pi} - \frac{sen(2.\phi_O)}{2.\pi}\right)} \qquad (17)$$

$$\overline{\overline{I_{D\_med1,2,3,4}}} = \frac{I_{D\_med1,2,3,4}}{I_{ref}} = D.\frac{\left(1-D.cos\phi_O\right)}{2\pi} \qquad (18)$$

$$\overline{\overline{I_{D\_RMS1,2,3,4}}} = \frac{I_{D\_RMS1,2,3,4}}{I_{ref}} = \frac{D}{2}.\sqrt{\frac{(1-D)}{2} + D.\left(\frac{\phi_O}{\pi} - \frac{sen(2.\phi_O)}{2.\pi}\right)} \qquad (19)$$

$$I_{ref} = \frac{V_{IN\_PK}}{\sqrt{2\left(R_O^{\ 2} + \left(2.\pi.f_R.L_O\right)^2\right)}} \qquad (20)$$

To simplify calculation, duty cycle *D* is changed by reference duty cycle D_{REF}. The most critical case occurs when D_{REF} is maximum (1,0) for all values of ϕ_O. Once these values have already known, and also V_{DC_PK}, it is simple to choose either IGBT or MOSFET, calculating conducing and switching losses.

Table II
Current on semiconductors

v_{IN_RMS}	*Inverter*				*Rectifier*
	I_{S_med}	I_{S_rms}	I_{D_med}	I_{D_rms}	I_{DR_rms}
110V	1,93A	3,51A	0,48A	1,43A	4,61A
220V	1,57A	3,12A	0,84A	2,15A	2,42A

Regarding the input rectifier, the input current dependence to the parameters given in (11) makes difficult to obtain an analytical solution, so a better one is through simulations.

The current on inverter switches and on rectifier diodes is shown in Table II. Each semiconductor was designed to attend the worst situation.

Finally, inductor L_{IN} was calculated to attend the stability criteria given in (21):

$$100.f_R \le f_O \le 4 \qquad (21)$$

So, f_O was chosen considering a resonance frequency of 6,8kHz. Finally, L_{IN} found is:

$$L_{IN} = \frac{1}{\left(2\pi.6,8k\right)^2.4,5\mu} = \boxed{121,7\mu H} \qquad (22)$$

That is commonly the order of line stray inductances. Its effects in this case are enough to eliminate the highest harmonic content. The low frequency order harmonics remains, as a drawback of this topology. A linear control structure was used attending the specifications in Table I. The details concerning its design have been briefly presented, and a more detailed explanation can be found in [12].

IV. EXPERIMENTAL RESULTS

In Fig. 7 and Fig. 8 two different situations are presented. Fed voltage is $220V_{RMS}$ in both. Load power (P_O) and $cos(\phi_O)$ are different.

The voltage V_{DC_PK} found is in accordance with (4), (5) and (6), such as with the methodology used for DC link capacitor determination. Besides, the different phase angle of input current (ϕ_{IN}) proves the behavior of a power factor correction element, in according to (7), (8) and (9), due to the angle α_{DC} additions. As it can be viewed, the input current has the sinusoidal waveform, so high frequency harmonic components were eliminated. Additionally, there is no resonance effect of the L_{IN}-C circuit composed by the capacitor and input inductance, as well as it was expected. This way, the input current total harmonic distortion (THD) is related mainly to the blocking angle of input rectifier. In Fig. 9, the converter operation with low harmonic current distortion and high power factor on the input side ($cos(\phi_{IN}) \ge 0,92$) is presented. It must be noted that $cos(\phi_O)$ is 0,78, which means an angle ϕ_O about 37,8º. In this case, the power load was reduced as like as the angle ϕ_O, and consequently, angle ϕ_{IN} was also reduced, improving the power factor of the structure. This proves that the converter can operates with a high power factor in the input, depending on parameters given in (7). Varying the load, Z_O was modified in the equation. Hence, it is possible to determine the value of Z_C, and finally of C, to obtain this condition. Certainly, the condition given in (5) should be respected. In spite of this, that was not the methodology used for converter design, but just the equations concerning the project parameters, what means (4) and (6).

The dominant losses are the commutation ones. The converter efficiency was about 91,7%. It is a good efficiency, but it could be improved because the converter was not optimized in terms of components. The main components used in prototype were:

(4x) IRFP27N60K - Output Switches (IR).
(3x) B32654A6155J - DC Link Capacitors (EPCOS).
(2x) AD734 -Analog Divider/Multiplier (Analog Devices).

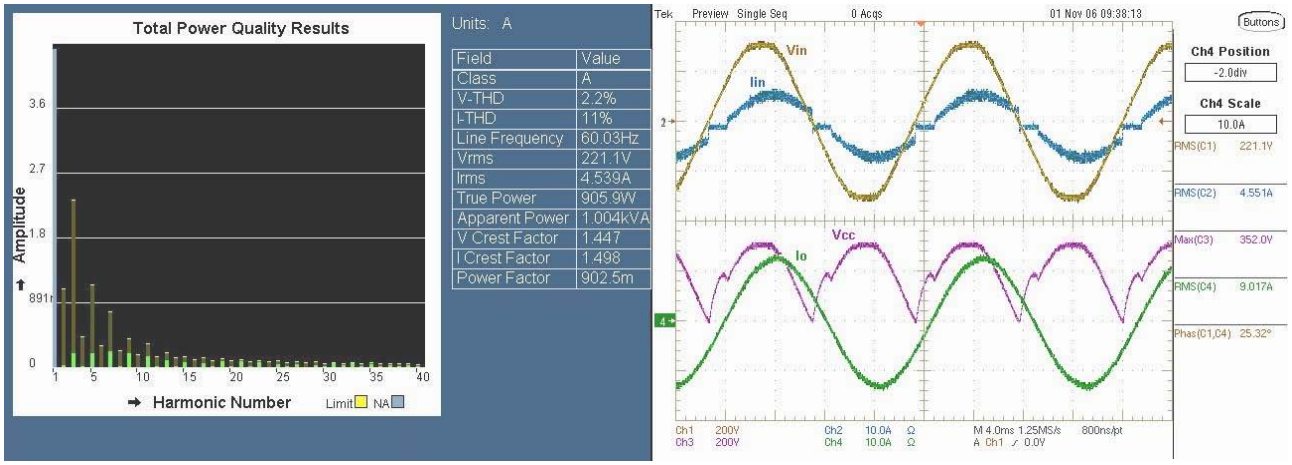

Fig. 7 – Harmonic analysis of input current (a) and waveforms (b) to $P_O \cong 900W$ and $cos(\phi_O) = 0,90$.

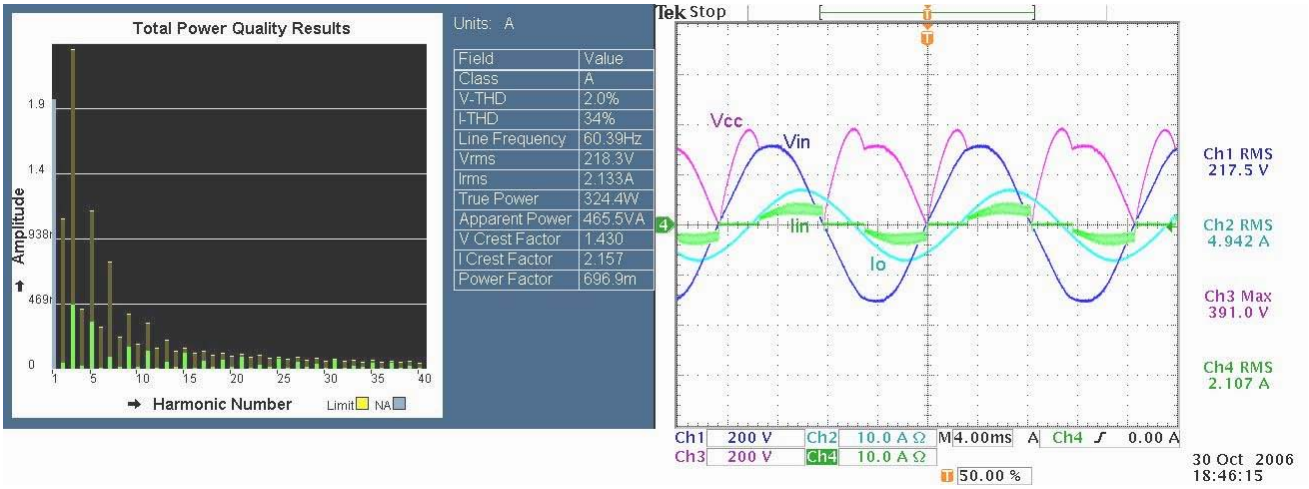

Fig. 8 – Harmonic analysis of input current (a) and waveforms (b) to $P_O \cong 325W$ and cos $(\phi_O) = 0,60$.

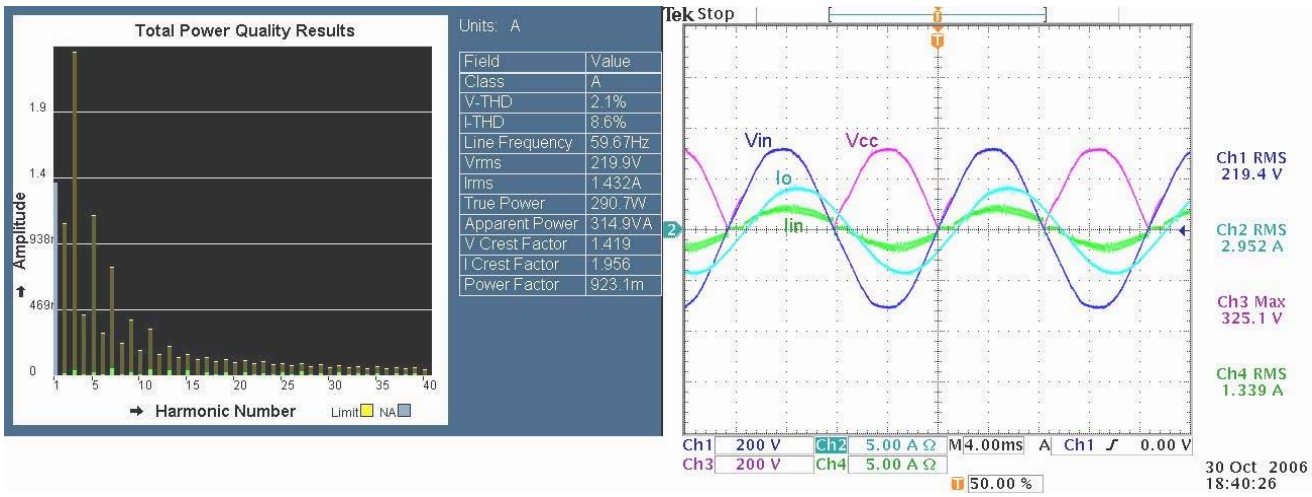

Fig. 9 – Harmonic analysis of input current (a) and waveforms (b) to $P_O \cong 300W$ and cos $(\phi_O) = 0,78$.

V. CONCLUSION

This paper presented the design methodology of an AC-AC converter, focusing on the power stage. The load, which is supposed to be a single-phase induction motor used in household appliances, was modeled as an RL circuit. The main characteristics and its implications were discussed. The control objective is regulating output voltage, in the case that

the device be used in systems with different supply voltages. The experimental results prove the ideas discussed.

ACKNOWLEDGEMENTS

The authors would like to thank for CAPES by financial support given during two years of research.

REFERENCES

[1] Claus B. Rasmussen; Ewen Ritchie; Antero Arkkio. *Variable Speed Induction Motor Drive for Household Refrigerator Compressor*. Proceedings of the IEEE International Symposium on Industrial Electronics (ISIE'97), Vol. 2, Nº 7-11, July 1997, pp. 655-659.

[2] B. –H. Kwon; B. –D. Min; J. -H Kim. *Novel Topologies of AC Choppers*. IEE Proceedings Electric Power Applications, Vol. 143, Nº 4, July 1996, pp. 323-330.

[3] Takayuki Shinyama; Akiteru Ueda; Akihiro Torri. *AC Chopper Using Four Switches*. Proceedings of the Power Conversion Conference (PCC 2002), April 2002, pp. 1056-1060.

[4] Nabil Abd El-Latif Ahmed; Kenji Amei; Masaaki Sakui. *Improved Circuit of AC Choppers for Single-Phase Systems*. Proceedings of the Power Conversion Conference (PCC 1997), August 1997, pp.907-912.

[5] Sadeq A. Hamed. *Steady-State Modeling, Analysis, and Performance of Transistor-Controlled AC Power Conditioning Systems*. IEEE Transactions on Power Electronics, Vol. 5, Nº 3, July 1990, pp. 305-313.

[6] P. N. Enjeti; Sewan Choi. *An Approach to Realize Higher Power PWM AC Controller*. Applied Power Electronics Conference and Exposition (APEC'93), March 1993, p. 323-327.

[7] B. –H. Kwon; B. –D. Min; J. -H Kim. *Novel Commutation Technique of AC-AC Converters*. IEE Proceedings Electric Power Applications, Vol. 145, Nº 4, July 1998, pp. 295-300.

[8] Joohn Sheok Kim; Seung Ki Sul. *New Control Scheme for AC-DC-AC Converter without DC Link Electrolytic Capacitor*. IEEE Power Electronics Specialists Conference (PESC'93), June 1993, pp. 300-306.

[9] L. Malesani; L Rossetto. et al. *AC/DC/AC PWM Converter with Reduced Energy Storage in the DC Link*. IEEE Transactions on Industry Applications, Vol. 31, Nº 2, March-April 1995, pp287-292.

[10] Henrik Kragh. *On the Control of a DC-Link High Frequency AC-Voltage Regulator*. Power Electronics Specialists Conference (PESC'01), IEEE 32nd Annual, vol. 2, Jun. 2001, pp. 1122-1128.

[11] Luis Cândido Tomaselli. *Study of Variable Speed Electrical Drive for Permanent Split Capacitor Single-Phase Induction Motors used in Blowers*. Florianópolis, SC – Brasil, 2004. Doctor Thesis – Power Electronics Institute (INEP), Federal University of Santa Catarina (UFSC).

[12] Romeu Antunes Friedemann. *AC-AC Converter for Household Appliances Fed by Wide Range Input Voltage*. Florianópolis, SC – Brasil, 2007. Master Dissertation – Power Electronics Institute (INEP), Federal University of Santa Catarina (UFSC).,

[13] B. –D. Min; B. –H. Kwon. *Novel PWM Line Conditioner with Fast Output Voltage Control*. IEE Proceedings Electric Power Applications, Vol. 145, Nº 2, March 1998, pp. 85-91.

[14] Yasuhiro Okuma. *PWM Controlled AC Power Supply Based on AC Chopper Technology and Its Applications*. Transactions IEE Japan, Vol. 119-D, Nº 3, 1999, pp. 412-419.